BIOCHEMISTRY
including biophysical chemistry & molecular biology
Article

Biochemistry **2009,** *48,* 10705–10715 10705
DOI: 10.1021/bi901016n

Kinetic Analysis of the Genome Packaging Reaction in Bacteriophage λ†

Qin Yang,‡ Carlos E. Catalano,§ and Nasib Karl Maluf*,‡

‡*Department of Pharmaceutical Sciences, School of Pharmacy, University of Colorado Denver, C238-P15, 12700 East 19th Avenue, Aurora, Colorado 80045, and* §*University of Washington School of Pharmacy, H172 Health Science Building, Box 357610, Seattle, Washington 98195-7610*

Received June 16, 2009; Revised Manuscript Received September 16, 2009

ABSTRACT: Bacteriophage λ is a double-stranded DNA virus that infects the *Escherichia coli* bacterium. λ genomic DNA is replicated via rolling circle replication, resulting in multiple genomes linked head to tail at the *cos* site. To insert a single λ genome into the viral capsid, the λ terminase enzyme introduces symmetric nicks, 12 bp apart, at the *cos* site, and then promotes a strand separation reaction, releasing the tail end of the previous genome and leaving a binary complex consisting of λ terminase bound to the head end of the adjacent genome. Next, the genome is translocated into the interior of the capsid particle, in a process that requires ATP hydrolysis by λ terminase. Even though DNA packaging has been studied extensively, currently no bulk assays are available that have been optimized to report directly on DNA translocation. Rather, these assays are sensitive to assembly steps reflecting formation of the active, DNA packaging machine. In this work, we have modified the DNase protection assay commonly used to study DNA packaging in several bacteriophage systems, such that it reports directly on the kinetics of the DNA packaging reaction. We have analyzed our DNA packaging data according to an *N*-step sequential minimal kinetic model and have estimated an overall packaging rate of 119 ± 8 bp/s, at 4 °C and 1 mM ATP. Furthermore, we have measured an apparent step size for the this reaction (m_{obs}) of 410 ± 150 bp. The magnitude of this value indicates that our assay is most likely sensitive to both mechanical steps associated with DNA insertion as well as occasional slow steps that are repeated every >410 bp. These slow steps may be reflective of the pausing events observed in recent single-molecule studies of DNA packaging in bacteriophage λ [Fuller, D. N., et al. (2007) *J. Mol. Biol. 373*, 1113−1122]. Finally, we show that either ATP or ADP is required for terminase cutting at *cos*, to generate the active, DNA packaging complex.

Double-stranded (ds) DNA viruses such as adenovirus, the herpes viruses, and several bacteriophages are composed of viral DNA tightly packaged within an icosahedral protein shell called the capsid (*2*−*5*). A critical step in the assembly of an infectious virus particle is packaging of viral DNA into the capsid, a process catalyzed by enzymes called terminases (*6*). For bacteriophage λ, DNA packaging has been studied extensively at the biochemical and genetic levels and presents an ideal system for understanding the role of terminase in DNA packaging. λ terminase is a multifunctional enzyme that possesses endonuclease, ATPase, strand separation, and ds DNA translocase activities (*6*). The enzyme coordinates these activities (1) to process viral DNA to form a nucleoprotein complex competent for DNA packaging and (2) to interact with the viral procapsid to package the genome (see Figure 1).

The λ terminase holoenzyme is composed of two proteins, called gpA and gpNu1, which assemble into a heterotrimer (gpA−gpNu1$_2$). The heterotrimer further assembles into a tetramer of heterotrimers, which is required to conduct its enzymatic activities. This tetramerization reaction is strongly stimulated by the presence of *Escherichia coli* host protein IHF[1] (*7*, *8*). IHF is a site-specific DNA binding protien that further bends the DNA up to 180° (*9*). Thus, it appears this DNA bending provides the heterotrimer with the appropriate architecture to promote assembly into the tetramer. The gpA subunit contains the enzymatic activities associated with the holoenzyme, while the gpNu1 subunit is responsible for specific recognition of the *cos* site (*5*).

Despite intensive study, few experiments that have been designed to look at only the λ terminase-catalyzed DNA packaging reaction, isolated from other assembly steps such as binding to the procapsids, have been performed. In particular, no bulk assays have been reported that have been optimized to yield information about the kinetic steps of the DNA packaging motor. In contrast to this, recent single-molecule experiments have been reported that have investigated the DNA packaging reaction in bacteriophage phi29, T4, and λ (*1*, *10*−*13*). While these experiments promise to yield deep insights into the DNA packaging mechanisms of the terminase motor proteins, quantitatively rigorous bulk assays are required for a complete characterization of the packaging reaction.

In this work, we have redesigned the bulk, DNA packaging assay available for the bacteriophage λ system (*14*), such that it reports directly on the genome packaging reaction. We have

†This work was supported by start-up funds provided by the Department of Pharmaceutical Sciences at the University of Colorado Denver School of Pharmacy.

*To whom correspondence should be addressed: Department of Pharmaceutical Sciences, School of Pharmacy, University of Colorado Denver, C238-P15, 12700 E. 19th Ave., Aurora, CO 80045. Phone: (303) 724-4036. Fax: (303) 724-2627. E-mail: karl.maluf@ucdenver.edu.

[1]Abbreviations: NLLS, nonlinear least-squares; *cos*, cohesive end site; IHF, integration host factor; complex I, binary complex formed between terminase and the matured, left end of the *cos* site; complex II, ternary complex formed between complex I and the viral capsid.

Published on Web 09/30/2009

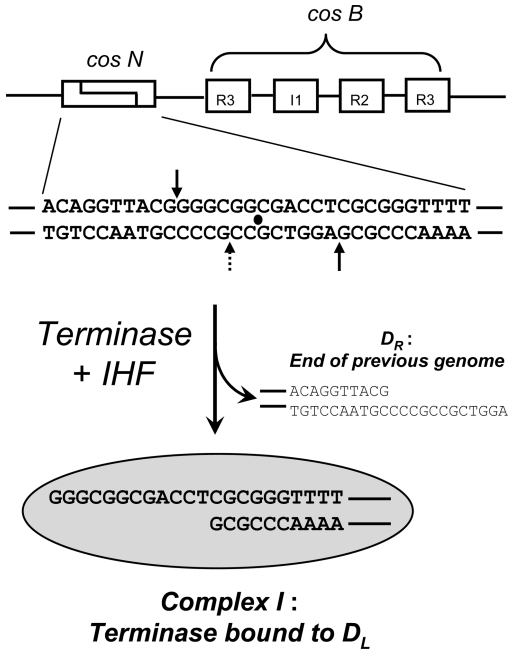

FIGURE 1: Schematic of the current model for the maturation process catalyzed by λ terminase. λ terminase binds to the *cos* site, which represents the site at which individual λ genomes are linked head to tail (*5*). Specific recognition of *cos* occurs through site-specific binding of the gpNu1 subunit to *cosB*, while the nicking reaction occurs at *cosN*. Symmetric nicks are introduced into the top and bottom strands by the gpA subunit of λ terminase, in a reaction whose rate and fidelity appear to be controlled by either ATP or ADP binding (solid arrows). In the absence of nucleotides, but in the presence of Mg^{2+}, the nick on the bottom strand is shifted 8 bp to the left (dashed arrow). Next, λ terminase promotes strand separation of the intervening 12 bp of ds DNA present between the two nicks. Upon strand separation, λ terminase remains associated with the D_L end, which represents the beginning of a genome: this is termed complex I.

further implemented a mathematical model that allows quantification of fundamental kinetic parameters of the packaging reaction, including the bulk packaging rate of the terminase motor, and have provided a quantitative framework with which to interpret the bulk measurement of the kinetic step size. The implications of this work with respect to the mechanisms of viral genome packaging are discussed.

EXPERIMENTAL PROCEDURES

Reagents. LB broth and LB agar were purchased from Fisher Scientific. Restriction enzymes were purchased from New England Biolabs. DEAE-Sepharose FF and SP-Sepharose FF chromatography resins were purchased from GE Healthcare. Nucleotides were purchased from Roche.

Protein Purification. Purification of hexahistidine-tagged terminase holoenzyme was performed as previously described (*15*). *E. coli* integration host factor was purified from overexpressing strain HN880 using the method of Nash et al. (*16*). Procapsids were expressed and purified as described previously (*14*).

Construction of the DNA Packaging Substrates. Three plasmids were used to generate the DNA substrates: pCTλ (*17*), in which an EcoRI−BamHI fragment (λ DNA sequence nucleotide 4972 of the 3′ end to nucleotide 5505 of the 5′ end) was cloned into pGEM-9Zf(−); pQY101, in which a λ fragment from nucleotides 5505−7910 was PCR amplified and cloned into the BamHI and SalI sites of pCTλ; and pQY102, in which the λ DNA sequence from nucleotide 5505 to 10410 was PCR amplified and cloned into the BamHI and SalI sites of pCTλ. These three DNA plasmids were subjected to the following restriction enzyme digestions to generate a series of lengths of the D_L fragments, after cleavage by λ terminase: (1) RsrII digestion of pCTλ which generated the D_L fragment of 3799 bp, (2) BamHI digestion of pCTλ which generated the D_L fragment of 5504 bp, (3) ScaI digestion of pCTλ which generated the D_L fragment of 7553 bp, (4) ScaI digestion of pQY101 which generated the D_L fragment of 9953 bp, and (5) ScaI digestion of pQY102 which generated the D_L fragment of 12453 bp.

DNA Packaging Reaction. In vitro DNA packaging was conducted as described previously (*14*, *18*) with modifications. The DNA packaging reaction consisted of three steps. Step 1 was generation of complex I by *cos* cleavage. The DNA substrate (29.4 nM) was incubated in 61.4 mM Tris (pH 8.0 at 23 °C), 9.1 mM β-mercaptoethanol, 2.35 mM spermidine, 11.8 mM $MgCl_2$, 17.6 mM NaCl, 4.9% glycerol, 58.8 nM *E. coli* integration host factor, 235 nM terminase (concentration expressed in terms of the gpA subunit), and the required ADP concentration to yield a final ADP concentration as indicated in the text. For example, to achieve a final ADP concentration of 0.05 mM, we included ADP at 0.059 mM in step 1. The reaction was initiated via addition of terminase and was conducted at 37 °C for 30 min. Step 2 was preincubation of complex I with procapsids and generation of complex II. Procapsids were added to a final concentration of 40 nM, at the end of the *cos* cleavage reaction, and were incubated for 5 min at 23 °C followed by 5 min at 4 °C. Upon addition of procapsids, the resulting solution conditions for this step were as follows: 25 nM DNA substrate, 55.2 mM Tris (pH 8) at 23 °C, 8.82 mM β-mercaptoethanol, 2 mM spermidine, 12.3 mM $MgCl_2$, 15 mM NaCl, 4.2% glycerol, 50 nM IHF, and 200 nM terminase. Step 3 was DNA packaging. ATP was added, from a concentrated stock, to the complex I/procapsid mixture, to a final concentration of 1 mM, and the packaging reaction was allowed to proceed at 4 °C. To stop the packaging reaction, an aliquot was transferred at the desired time points to a stop solution, which contained DNase I, $MgCl_2$, and ADP, resulting in final concentrations of 10 μg/mL, 10 mM, and 5 mM, respectively (the final ADP concentration, upon quenching, was 10 times greater than the final ATP concentration). The unpackaged DNA was digested away by DNase I at 23 °C for 5 min. The reaction mixture was extracted with a phenol/chloroform mixture, and the aqueous phase was removed and electrophoresed through a 1% agarose gel. The amount of DNA packaged was visualized by ethidium bromide staining and quantified by video densitometry analysis as previously described (*14*). The final solution conditions under which the DNA packaging reaction was performed were identical to those reported for step 2.

Analysis of Experimental Data. The DNA packaging experiments were analyzed according to Scheme 1, as described in Results. The time dependence of the fraction of DNA packaged according to Scheme 1 is given by eq 1 (*19*):

$$F(t) = A_T\left(1 - \frac{\Gamma(N,kt)}{\Gamma(N)} - e^{-k_{NP}t}(1-x)\left(\frac{k}{k-k_{NP}}\right)^N \left\{1 - \frac{\Gamma[N,(k-k_{NP})t]}{\Gamma(N)}\right\}\right) \quad (1)$$

where N is the total number of steps taken by the motor, k is the packaging rate constant (units of time^{-1}), k_{NP} is the rate constant

Scheme 1

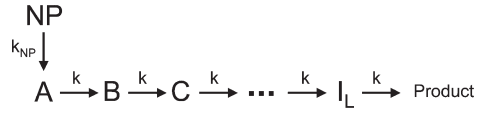

for formation of the productive ternary complex from the assumed nonproductive ternary complex (time^{-1}), x is the fraction of the productive ternary complex that exists at equilibrium, before ATP is added to start the packaging reaction, A_T is the reaction amplitude, and t is the reaction time. In eq 1, $\Gamma(N)$ and $\Gamma(N,kt)$ are the Γ function and incomplete Γ function, respectively (*19*). According to Scheme 1, the step size of the processive DNA packaging reaction, m, is defined as the total number of base pairs that are packaged per cycle of the motor (i.e., upon progression of the I_{n-1} intermediate to the I_n intermediate). With this definition, N is given by $N = L/m$, where L is the entire length, in base pairs, of the DNA that is packaged.

In our hands, even though we routinely use eq 1 to analyze data for which $N < 250$, we were unable to use eq 1 to simulate data that potentially contained a large number of total steps ($N >$ 250 steps), apparently due to computer round-off errors when calculating the ratio of Γ functions. To circumvent this technical difficulty, the terms in eq 1 that contain the Γ functions, i.e., $1 - \Gamma(N,kt)/\Gamma(N)$ and $1 - \Gamma[N,(k - k_{NP})t]/\Gamma(N)$, were replaced with the integrated Gaussian distribution, yielding eq 2:

$$F(t) = A_T(\Phi(N,kt) - e^{-k_{NP}t}(1-x)\{k/(k-k_{NP})^N \Phi[N,(k-k_{NP})t]\}) \quad (2)$$

where $\Phi(N,k_{app})$ is given by eq 3:

$$\Phi(N,k_{app}t) = \frac{k_{app}}{\sqrt{2\pi N}}\int_0^t e^{-(k_{app}t-N)^2/2N}\,dt \quad (3)$$

and k_{app} refers to either k or $(k - k_{NP})$ from eq 1. It can be shown that this substitution is exact in the limit of $N \rightarrow \infty$. For the purposes of NLLS analysis, we find no significant differences when analyzing simulated data that contain $N > 50$ using either eq 1 or 2.

The data were analyzed by nonlinear least squares (NLLS) methods using the software packages Scientist (Micromath) and Conlin (*20*). Monte Carlo simulations were performed to determine the experimental uncertainties on the fitted parameters using Conlin, and the uncertainties correspond to the standard deviations of the generated distributions.

RESULTS

Development of an Assay for Measuring DNA Packaging Kinetics. The standard assay that has been employed to investigate DNA packaging has taken advantage of the fact that packaged viral DNA is rendered resistant to digestion by DNase (*14*, *18*, *21*, *22*, *24*, *25*), since it cannot access the packaged DNA due to the protective capsid. For bacteriophage λ, an in vitro DNA packaging assay has been developed that uses only purified components; λ procapsids and terminase are purified to homogeneity as described, as well as additional accessory proteins that are also involved in the DNA packaging reaction (*14*, *18*, *23*).

However, previous studies that have looked at the DNA packaging kinetics using the DNase protection assay were not designed for investigation of the kinetics of the actual packaging reaction, i.e., the kinetic step(s) associated with the terminase enzyme translocating the DNA into the capsid. Previous assays, for a number of different phage systems, typically initiate the packaging reaction by addition of the terminase enzyme (*14*, *22*, *24*, *25*). Thus, these kinetic experiments are sensitive to the assembly kinetics of the terminase, DNA, and procapsid.

To circumvent these problems, we have isolated the DNA packaging kinetics from the assembly kinetics by redesigning the in vitro DNase protection assay as follows. First, λ terminase, along with 1 mM ADP, is incubated at 37 °C for 30 min, with a cloned linear DNA fragment that contains an intact *cos* site (Figure 1). Upon cleavage of the *cos* site in this particular DNA fragment (see Experimental Procedures), a 7.6 kb substrate is generated. This reaction, known as the *cos* cleavage reaction, generates complex I, which corresponds to λ terminase bound to the matured left end of the 7.6 kb DNA fragment. This complex is very stable, with a half-life of >8 h (*26*). Next, λ procapsids are incubated with the newly generated complex I at 23 °C for 5 min. Incubation times up to 10 min yielded identical results. During this time, complex I and procapsids associate with each other, forming the active ternary complex (terminase, DNA, and procapsids, represented as A in Scheme 1, which is termed complex II in the literature) that is poised to rapidly begin DNA packaging upon addition of ATP. The packaging reaction is initiated by addition of 1 mM ATP and stopped at various times by addition of DNase to a final concentration of 10 μg/mL. The DNase reaction mixture is incubated for 5 min to digest any DNA external to the capsid, and the reaction is stopped by addition of a phenol/chloroform mixture, which also serves to extract the packaged DNA from the interior of the capsid. The aqueous phase, containing the extracted DNA, is electrophoresed through a 1% agarose gel. The DNA is visualized by ethidium bromide staining, and the amount of DNA packaged is quantified by densitometric analysis using ImageQuant, as reported previously (*14*). Control experiments show the amount of DNA loaded on the gel in our experiments is within the linear range of the instrument (data not shown).

In the experimental design described above, we used ADP rather than ATP to promote the *cos* cleavage reaction and generate complex I. This allowed us to incubate complex I with procapsids, generating complex II, under conditions where no DNA packaging would take place, since the packaging reaction requires ATP hydrolysis (*14*). This obviates the need to quantitatively account for the assembly kinetics of complex II formation when analyzing the DNA packaging kinetics. The ability to carry out the *cos* cleavage reaction in the presence of ADP, rather than ATP, is discussed in a later section.

Figure 2A shows an image of an agarose gel in which the DNA packaging reaction time (the time between addition of ATP and addition of DNase) has been varied from 15 s to 20 min, and Figure 2C shows the quantification of the same results, presented as the total concentration of full-length (7.6 kb) DNA that has been packaged. In stark contrast to previously published DNA packaging time courses (*14*), we see that for the first 15 s time point, approximately 50% of the plateau value of total DNA packaged has been reached. This implies a packaging rate of roughly 500 bp/s (7.6 kb/15 s $\cong$ 500 bp/s), at 23 °C, in 1 mM ATP and 1 mM ADP, much faster than the previously estimated value of ~35 bp/s (using the data in Figure 4 of ref *14*). We can compare our number to the value reported by Smith and co-workers of ~600 bp/s, at 23 °C, measured using single-molecule methods to study DNA packaging in bacteriophage λ (*11*). However, this value was obtained by specifically editing out events such as

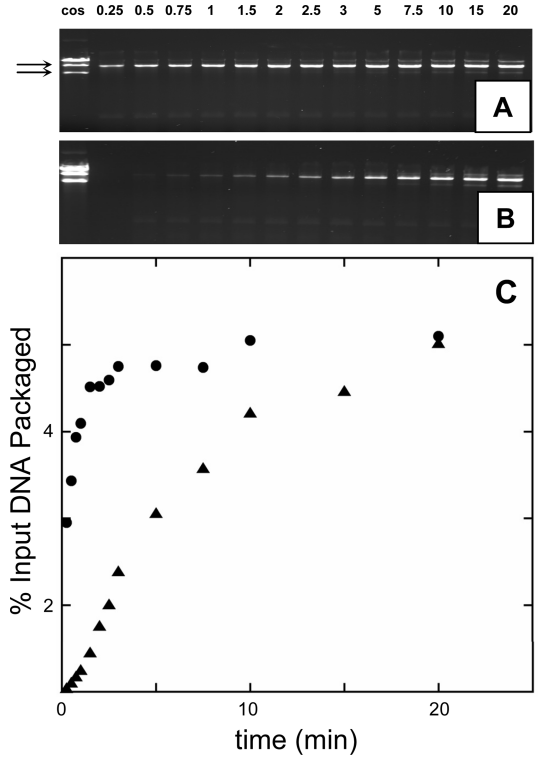

FIGURE 2: (A) The first lane shows the *cos* cleavage reaction, conducted in the presence of 1 mM ADP for 30 min, which generates complex I. The top arrow shows the 7.6 kb D_L fragment, while the bottom arrow shows the 4.7 kb D_R fragment. Procapsids were then incubated for 5 min, after which the DNA packaging reaction was initiated by addition of 1 mM ATP. The reaction was quenched at various times, shown above the gel (in minutes). (B) The *cos* cleavage reaction was conducted in the presence of 1 mM ATP for 30 min. The DNA packaging reaction was then initiated by addition of procapsids. (C) The data in panels A and B were quantified by gel densitometry and are plotted in panel C.

motor pausing from the single-molecule data. To compare our value estimated using bulk kinetic approaches to the value obtained from the single-molecule experiments, we need to include events such as pausing. When these events are included, we estimate a value of 469 bp/s from the single-molecule data, very similar to our estimate of ~500 bp/s. We will present this calculation in more detail in the Discussion.

Figure 2 also shows a comparison of DNA packaging kinetics conducted as described above (with procapsid preincubation) with a reaction that was performed without procapsid preincubation. Terminase was incubated with the 7.6 kb DNA packaging substrate along with 1 mM ATP, for 30 min at 37 °C, after which the packaging reaction was initiated by addition of procapsids. In this experiment, the association kinetics of the binding of the procapsid to complex I are clearly evident because of (1) the increased time it takes to observe the fully packaged 7.6 kb DNA substrate and (2) the presence of a small lag phase, which indicates the existence of at least one intermediate along the assembly reaction pathway, which most likely corresponds to the formation of complex II. It is important to note this lag phase does not arise due to repeated rounds of DNA packaging but rather arises due to the time required to first form the active ternary complex. This is clear since the DNA packaging kinetics are much faster when they start from the preformed complex II.

Kinetic Analysis of the Genome Packaging Reaction. The *N*-step sequential scheme (Scheme 1) has been used extensively to analyze a range of protein translocation processes, especially helicase translocation and DNA unwinding (*27*). In this scheme, a protein translocase is envisioned that moves along a linear lattice such that it translocates *m* lattice units for every kinetic step it takes. In the context of our DNA packaging experiments, a direct prediction of the *N*-step sequential kinetic scheme is that there will be a lag phase present in the DNA packaging time courses, and the extent of this lag phase will increase with an increase in the length of the DNA packaging substrate. However, it is clear that under our current conditions, the DNA packaging reaction is too fast to observe a lag phase (Figure 2C). Therefore, to slow the packaging reaction, we decreased the temperature to 4 °C. Second, we were concerned that the DNA packaging reaction may be sufficiently fast that a significant amount of packaging could still occur before the external DNA was completely digested during the DNase quench reaction. To address this concern, we included a 10-fold excess of ADP along with the DNase quench solution. Thus, the excess ADP could compete with ATP for the ATPase sites on the terminase motor, significantly slowing the packaging reaction so that the DNase could digest the DNA external to the capsid much more rapidly than the DNA could be inserted into the capsid interior. Control experiments confirmed that no packaging was observed under these conditions for up to 20 min, showing these concentrations are sufficient to stop the packaging reaction during the DNase digestion (see Figure 4).

Figure 3A shows an image of an agarose gel that represents a DNA packaging time course performed at 4 °C and quenched with elevated concentrations of ADP. Importantly, for the early time points examined, smears that correspond to DNA fragments shorter than 7.6 kb are present and, thus, show directly the presence of partially packaged DNA intermediates. Further, at later times, the average size of the intermediates increases until finally enough time has elapsed so that the full-length 7.6 kb DNA substrate has been completely packaged. These results are qualitatively consistent with the behavior predicted by the simple *N*-step sequential mechanism presented in Scheme 1. Previously, Duffy and Feiss (*28*) isolated mutants of the *A* gene which resulted in a stalled DNA packaging phenotype, thus providing direct evidence for partially packaged DNA intermediates in the bacteriophage λ system. Now, for the first time, we have obtained evidence of partially packaged DNA intermediates using an in vitro, bulk, kinetic assay.

These results were quantified by only counting the band corresponding to packaging of the full-length, 7.6 kb DNA substrate. Thus, any partially packaged DNA intermediates, whose lengths are shorter than 7.6 kb, are not counted in this analysis. By analyzing the data this way, we expect to see a time course that displays a lag phase, which represents the average amount of time it takes, starting from the active ternary complex (complex II), to package the entire 7.6 kb DNA substrate. These results are plotted in Figure 3B. Figure 3B shows the early region of the time course, while Figure 3C shows the full time course. As expected, the time course displays an obvious lag phase. However, the data also indicate a significant second, slower phase.

We interpret these data to indicate that a fraction of complex II partitions into a nonproductive complex that is in equilibrium with a packaging-competent complex; that is, complex II exists as two different species, one that is poised to rapidly package the DNA (represented by A in Scheme 1) and another that must first undergo a slow kinetic step to form the productive species, after which it can rapidly package the DNA (represented by NP in

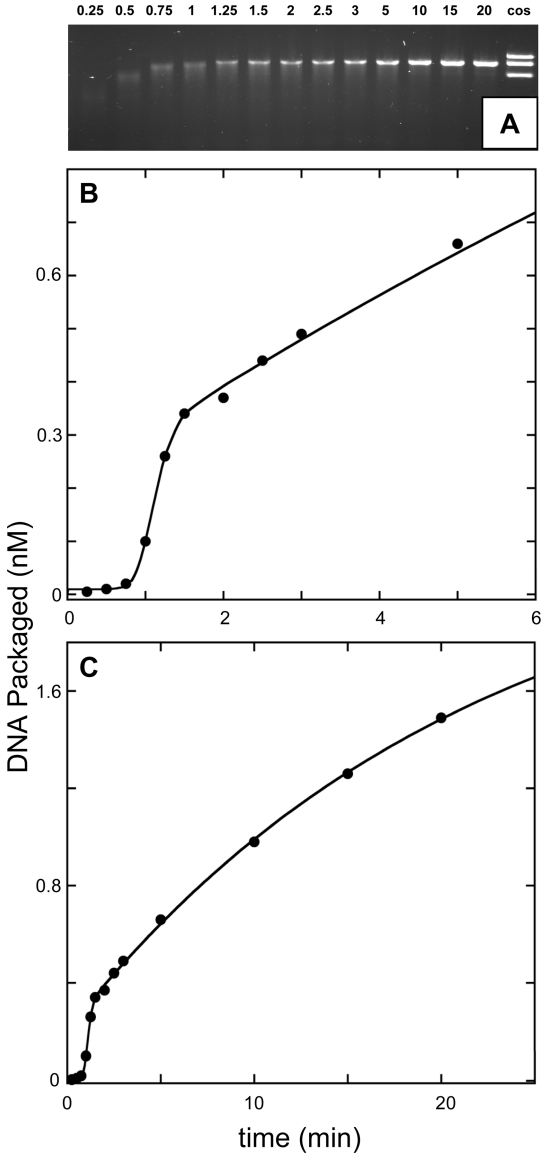

FIGURE 3: (A) Agarose gel showing a time course for DNA packaging of the 7.6 kb DNA substrate, at 4 °C, with 10 mM ADP included in the DNase quenching solution. The time point is shown above each lane (in minutes). The *cos* cleavage reaction was conducted in the presence of 1 mM ADP, for 30 min at 37 °C. Partially packaged intermediates are obvious as smears at the earlier time points. (B) The data in panel A were quantified by densitometric analysis of the full-length, 7.6 kb packaged product, and the early time points are shown. (C) The full time course is shown. The smooth curves in panels B and C are simulations generated using eq 1 along with the best fit parameters derived from the NLLS analysis of the data. The best fit parameters are given in the text.

Scheme 1). Thus, the lag phase results from the fraction of complex II that is poised to rapidly package the DNA, while the slow phase results from complex II that must first undergo a slow rearrangement before entering the rapid packaging phase. This interpretation is consistent with previous kinetic studies from our lab that similarly demonstrated a biphasic *cos* cleavage time course (*17*, *29*). Analysis of the data according to eq 1 indicates that the fraction of packaging-competent complex II, x, that exists at equilibrium before addition of ATP, is 0.130 ± 0.007 and that the rate constant for formation of this complex from the assumed nonproductive ternary complex, k_{NP}, is 0.046 ± 0.005 min^{-1}, at 4 °C, in 1 mM ATP and 1 mM ADP (Figure 3B,C). The rate constant, k, and the packaging step size, m, are not well-

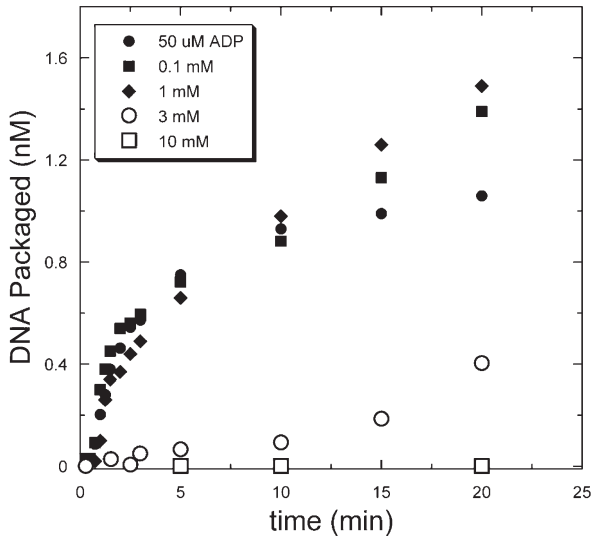

FIGURE 4: DNA packaging experiments were performed using the 7.6 kb packaging substrate, as described in the text. The dependence of the DNA packaging kinetics on the ADP concentration was investigated by varying the concentration of ADP used to generate complex I.

constrained in the fitting, due to excessive negative parameter correlation. However, the product k_{bps} ($=km$) is well-determined due to error cancellation (if k is overestimated, m tends to be underestimated and vice versa); analysis of the data yields a packaging rate for the fast phase, k_{bps}, of 113 ± 5 bp/s, at 4 °C, in 1 mM ATP and 1 mM ADP.

Since we designed our assay to use ADP to generate complex I, the DNA packaging phase of our experiments will also take place in the presence of ADP. Therefore, to examine the effect of ADP on the DNA packaging kinetics, we varied the ADP concentration used in the *cos* cleavage step of the reaction (step 1; see Experimental Procedures) to examine the effect of the carry-over ADP concentration on the packaging kinetics. We see that the fast, lag phase of the time course is essentially independent of the ADP concentration present during the *cos* cleavage and DNA packaging phases of the reaction, up to ~1 mM (Figure 4). However, for higher ADP concentrations, the packaging reaction is strongly inhibited; the presence of 3 mM ADP results in observable levels of packaging at ~10 min, while the presence of 10 mM ADP results in a complete inhibition of observable packaging up to at least 20 min. These results also indicate that addition of 10 mM ADP along with the DNase, in the quench solution, will effectively stop any further packaging that may occur during the time it takes for DNase to digest the DNA external to the capsid.

If our hypothesis is correct that the first phase observed for packaging the 7.6 kb DNA substrate reflects a population of active ternary complexes that are poised to begin rapid DNA packaging upon addition of ATP, then a prediction of this model is that the average time it takes to package a DNA substrate, during the lag phase of the packaging reaction, will be directly proportional to the DNA length, L. To test this prediction, we constructed four additional DNA substrates, such that after the *cos* cleavage reaction, DNA lengths of 3.8, 5.5, 10.0, and 12.5 kb are generated. These lengths are sufficiently short (the longest being only 26% of the total λ genome length) that any buildup in internal pressure inside the capsid, due to DNA packaging, can be ignored (see Figure 5 of ref *1*); i.e., we can assume the rate

constant, k, presented in Scheme 1, is constant throughout the entire packaging reaction.

The DNA packaging kinetics of these additional DNA substrates were measured as described above, and 0.05 mM ADP was used in the *cos* cleavage reaction to generate complex I. The resulting time courses are plotted in Figure 5B,C. Qualitatively, it is clear these additional DNA substrates all display lag phases and that, in general, the extent of the lag phase increases with an increase in DNA length, consistent with the N-step sequential scheme. These data were also analyzed using eq 1. Figure 5A shows a plot of the average time it takes to package each DNA substrate (given by $\mu = L/k_{bps}$), as a function of DNA length, L. As predicted by the N-step sequential scheme, μ is linearly related to L. The inverse of the slope from the LLS analysis of these data gives a k_{bps} of 113 ± 4 bp/s, at 4 °C, in 1 mM ATP and 0.05 mM ADP. This result is strong evidence that the first phase observed in the packaging kinetics for these DNA substrates is in fact a reflection of the actual packaging reaction, as opposed to other steps such as the binding of the procapsid to complex I. Furthermore, the linear dependence of μ on L also validates our assertion that there is not a buildup of significant internal pressure that will slow the motor while packaging these relatively short DNA lengths.

To further test the applicability of Scheme 1 to our packaging data, we analyzed the data shown in Figure 5B,C using global, NLLS methods. This analysis also allows us to estimate the apparent step size of the terminase motor (i.e., allows us to estimate m_{obs}, as defined in the Appendix), due to the increased quantity of data available to serve as constraints on the best fit parameters. In this analysis, we used eq 1 to analyze the length dependence of the packaging kinetics by setting k, m, k_{NP}, and x as global fitting parameters (constant for each of the five DNA lengths investigated), while allowing each data set to have its own (local) amplitude and baseline offset. The results of this analysis are shown as smooth curves in Figure 5B,C. The best fit parameters are as follows: $k_{bps} = 119 \pm 8$ bp/s, $k = 18 \pm 8$ min^{-1}, $m = 410 \pm 152$ bp, $k_{NP} = 0.21 \pm 0.01$ min^{-1}, and $x = 0.27 \pm 0.02$. We note here that our value for m is obviously too large to be interpreted as a mechanical step size; i.e., it is not possible a single mechanical process within the terminase motor (e.g., a protein conformational change) could be coupled to the insertion of 410 bp of DNA into the capsid interior. Furthermore, we note that the values for k_{NP} and x appear to depend on the ADP concentration, such that both values increase with a decrease in ADP concentration. This might indicate a role for ADP in partitioning between the productive (A) and nonproductive (NP) forms of complex II (Scheme 1); however, additional experiments are required to test this possibility.

Nucleotide Requirements for the Generation of Complex II. To generate complex II, we conducted the *cos* cleavage reaction in the presence of ADP, rather than ATP. We did this so that upon formation of complex II, the DNA packaging reaction would not be initiated, since no ATP would be available to support the reaction. This allows us to synchronize the packaging reaction such that packaging begins upon addition of ATP.

Previous studies (*30*) have investigated the nucleotide requirements for high-fidelity nicking and strand separation for processing *cos* by λ terminase. These studies were all conducted in the absence of the IHF protein. These studies showed that either ATP, ADP, AMP-PNP, or ATPγS was sufficient to promote high-fidelity nicking, introducing nicks in the top and bottom

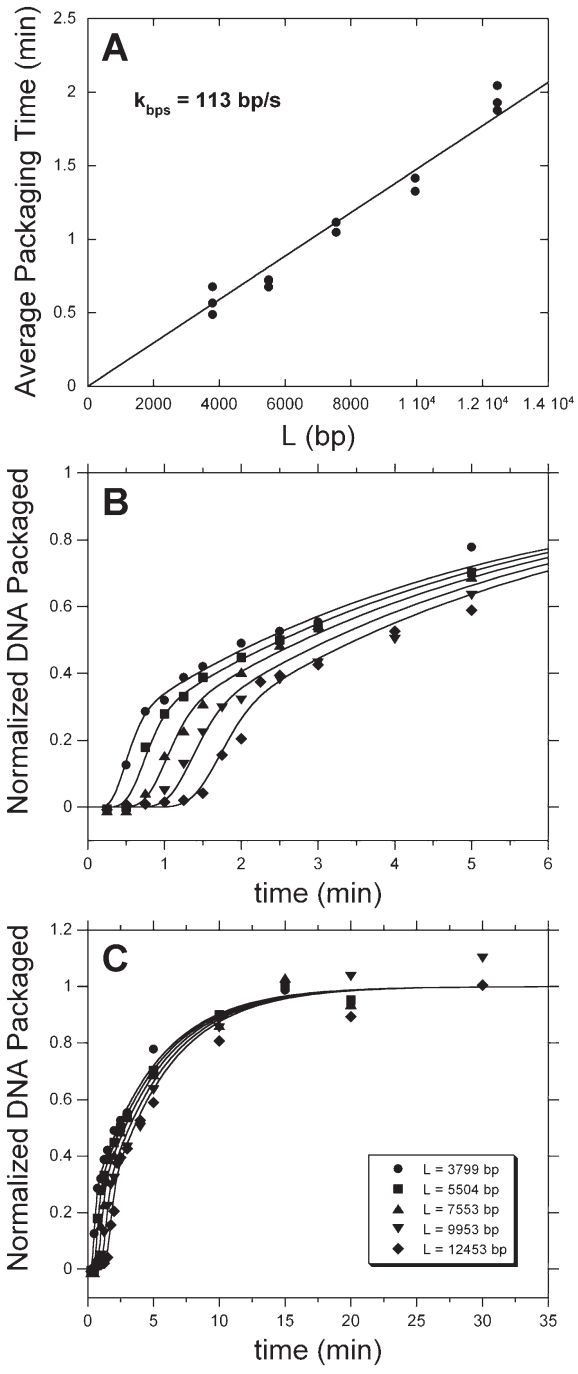

FIGURE 5: Effect of DNA packaging substrate length on packaging kinetics. Complex I was generated using 0.05 mM ADP, and upon generation of complex II by the addition of procapsids, the packaging reaction was initiated by addition of 1 mM ATP. (A) Five DNA lengths were investigated, as indicated in the figure. Each time course displayed two phases, a rapid lag phase and a second, slow phase. The average time (μ) it took to fully package each DNA length, during the rapid lag phase, was calculated as described in the text and plotted vs DNA length, L. As expected on the basis of Scheme 1, μ was linearly related to L. (B) Results of the global, NLLS analysis of each time course, using Scheme 1. Multiple time courses were collected for each DNA length, as follows: three time courses for the 3799 bp substrate, three time courses for the 5504 bp substrate (in panel A, two values of μ were identical), two time courses for the 7553 bp substrate, two time courses for the 9953 bp substrate, and three time courses for the 12543 bp substrate. The best fit results from this analysis are presented in panel B by averaging the time courses collected for each length. Overlaid on the experimental data are simulations generated using the best fit parameters. (C) Enlarged time scale showing the second, slower phase.

strands, with an intervening 12 bp of ds DNA between them (Figure 1). In the absence of the nucleotide cofactor, but in the presence of Mg^{2+}, the authors observed that nicking also occurred; however, while the nick on the top strand remained unchanged, the nick on the bottom strand was shifted 8 bp to the left, which resulted in 4 intervening base pairs between the top and bottom nicks (dashed arrow in Figure 1).

It is well-known that an annealed *cos* site, which possesses 12 complementary base pairs of ds DNA, will not spontaneously dissociate under physiological conditions. Thus, the authors investigated the nucleotide requirements for the subsequent λ terminase-catalyzed strand separation reaction. When the authors assayed for strand separation, rather than just the nick generation, they observed that the nonhydrolyzable nucleotide analogues ATPγS and AMP-PNP were unable to support the strand separation reaction. On the basis of this result, they concluded ATP hydrolysis was required to promote the strand separation reaction. However, the authors did not investigate the possibility that ADP binding alone was sufficient to promote the strand separation reaction.

In our experiments, we see that when the *cos* cleavage reaction is conducted in the presence of ADP, we observe the two cleavage products on the native agarose gel (see the lanes labeled *cos* in Figures 2 and 3). To explain this result, we consider that one of two possibilities has occurred. In the first scenario, λ terminase first conducted the high-fidelity nicking reaction, introducing two nicks 12 bp apart, and then separates the intervening 12 bp of ds DNA in an ADP-dependent fashion. The chemical nature of this strand separation is not clear. In the second scenario, λ terminase again introduces two nicks; however, the nick on the bottom strand is shifted 8 bp to the left, leaving only 4 bp of intervening ds DNA. It is well-known (*30*, *31*), and we have reproduced the result (see Figure S1 of the Supporting Information), that when the two matured ends of *cos* are annealed (resulting in a nicked *cos* site, containing 12 intervening base pairs of DNA between the two nicks), this complex remains associated during native agarose gel electrophoresis. Upon heating this complex for 5 min at 70 °C, we observe melting of the annealed DNA, as expected. However, it is not expected that 4 annealed base pairs of cDNA will be sufficient to hold the entire DNA molecule together during electrophoresis. Thus, according to the second scenario, we expect to observe two cleavage products on the native agarose gel due to the instability of the complex. Consistent with this, when we conduct the *cos* cleavage reaction in the absence of nucleotide cofactors, but in the presence of Mg^{2+}, conditions under which we might expect generation of the incorrect nick on the bottom strand (dashed arrow in Figure 1), we do see the cleavage reaction products on the agarose gel (Figure S2 of the Supporting Information). However, we also see both cleavage products when the *cos* cleavage reaction is conducted in the presence of ATPγS or AMP-PNP (Figure S3 of the Supporting Information), which is inconsistent with the previous conclusion that while ATPγS and AMP-PNP will support the high-fidelity nicking reaction (leaving 12 bp of annealed DNA between the nicks), they are unable to support the strand separation reaction. We have thought of three scenarios that can explain this observation. (1) ADP, ATPγS, and AMP-PNP do support high-fidelity nicking, and they also support the strand separation reaction. (2) ADP, ATPγS, and AMP-PNP do not support the high-fidelity nicking reaction, resulting in the generation of the incorrect nick on the bottom strand; thus, the remaining 4 bp of intervening DNA is not sufficient to hold the DNA molecule together during native agarose electrophoresis. (3) Since all our experiments were conducted in the presence of IHF, while the previous *cos* cleavage experiments (*30*) were conducted in its absence, IHF may play a role in promoting the strand separation reaction, such that ADP, ATPγS, and AMP-PNP can all support the strand separation reaction in its presence. We are currently testing these possibilities in our laboratories.

Since we were able to conduct a *cos* cleavage reaction in the absence of nucleotides, but in the presence of Mg^{2+}, we tested the possibility that we could generate complex II, the active DNA packaging complex, by processing *cos* in the absence of any nucleotide cofactors (Figure S2 of the Supporting Information). If we could generate complex II in this way, we would expect to observe DNA packaging upon subsequent addition of ATP. Surprisingly, we observe that when the *cos* site is first processed in the absence of nucleotide cofactors, we observe no subseqeunt DNA packaging. Increasing the incubation time (up to 30 min) of the procapsid addition step did not result in packaged DNA (data not shown). Furthermore, if the *cos* cleavage reaction was first conducted in the absence of ADP and then the mixture allowed to incubate for an additional 30 min in the presence of 1 mM ADP prior to procapsid addition, no DNA packaging was observed (data not shown). However, when *cos* is first processed in the presence of ATP, ADP, ATPγS, or AMP-PNP, we observe that the processed *cos* DNA can be packaged (Figure S3 of the Supporting Information). Thus, we conclude there is an absolute requirement for nucleotide cofactors for processing the *cos* site to generate a DNA packaging competent terminase−DNA−procapsid ternary complex. However, the molecular nature of this requirement is not known.

DISCUSSION

In this work, we have modified the DNase protection assay, commonly used to study DNA packaging in several bacteriophage systems (*14*, *18*, *21*, *22*, *24*, *25*), to specifically monitor the kinetics of the DNA packaging reaction. Previous attempts (*14*, *18*, *23*) to study the kinetics of the DNA packaging reaction in bacteriophage λ, when employing bulk assays utilizing the DNase protection assay, were complicated by the presence of additional assembly steps in the reaction. In the case of bacteriophage λ, it is now clear that the amount of time it took to assemble the active ternary complex, composed of terminase, procapsids, and mature λ DNA (also called complex II), is rate-limiting. This is obvious with a comparison of the DNA packaging kinetics when the reaction is conducted with and without procapsid incubation; when complex II is allowed to form before the DNA packaging reaction in initiated, the DNA packaging reaction proceeds much more rapidly than when the DNA packaging reaction is initiated by addition of procapsids (Figure 2C). The consequence of this is that the kinetics of the DNA packaging reaction could not be observed in these previous experiments, due to the slow rate of complex II assembly, which dominates the time course. The simple experimental design presented here should be amenable to other viral DNA packaging systems and will allow study of the kinetics of the DNA packaging reaction, separated from other assembly steps.

Biphasic DNA Packaging Kinetics. In our experiments, we observed two distinct phases in the DNA packaging kinetics. The first, rapid phase is a result of processive DNA packaging that contains an occasional slow step that repeats on average approximately >410 bp. We use the greater-than sign for the following

reason. One possibility is that the kinetics of the actual insertion of the DNA into the capsid are much faster than the kinetics of the slow step, such that the total time the motor spends packaging DNA is much shorter than the time it spends progressing through the slow step. If this is the case, then we can interpret the step size we measured as reflecting the repetition of a slow step on average every 410 bp; i.e., this value can be interpreted as the kinetic step size, m_{kss} (see the Appendix and Scheme 2). On the other hand, if the total time the motor spends packaging DNA is similar to the total time it spends progressing through the slow step, then we can conclude our measured step size m_{obs} of 410 bp is smaller than the kinetic step size, i.e., that $m_{kss} > 410$ bp.

To illustrate this point, we consider the elegant single-molecule experiments that were published studying DNA packaging for the λ terminase motor (*1*). At low forces (5 pN), the authors measured a DNA packaging rate of ~600 bp/s, at 23 °C. They also observed that the motor would occasionally pause, with a pausing frequency of 0.1 pause per second, and an average pause duration (the average time the motor spent in the paused state) of 2.8 s. Therefore, the slow step we observe in our bulk DNA packaging experiments may correspond to physical pausing of the λ terminase motor during DNA packaging. From the single-molecule data, we can calculate that the motor will pause on average once every 6000 bp (600 bp s^{-1}/0.1 pause s^{-1} = 6000 bp $pause^{-1}$) and that the rate constant that describes recovery from this paused state, k_p, is 0.36 s^{-1} (1/2.8 s = 0.36 s^{-1}). By looking at the effect of applied force on the packaging reaction, the authors determined the reaction is composed of at least two kinetic processes, one that is force-dependent and another that is force-independent. For the force-dependent kinetic process, the authors calculated a characteristic distance of close to 1 bp, suggesting this step of the motor is associated with the generation of a force over a distance of 1 bp, such that 1 bp is packaged per mechanical event within the motor. Therefore, at an applied force of 5 pN, there are at least two kinetically significant steps that occur per base pair of DNA that is packaged, and together, these two processes result in a total packaging rate of 600 bp/s. This corresponds to a total time of 1.67×10^{-3} s (1 bp/600 bp s^{-1} = 1.67×10^{-3} s) spent packaging a single base pair of DNA. According to the analysis of the force dependence of the DNA packaging velocity, at 5 pN applied force, the reaction velocities for these two kinetic steps are 410 and 190 bp/s (*1*). Thus, for every base pair packaged, the total time spent in the first kinetic step, $1/k_1$, is given by $(1 - 410/600) \times 1.67 \times 10^{-3}$ s = 5.29×10^{-4} s, while the total time spent in the second kinetic step, $1/k_2$, is given by $(1 - 190/600) \times 1.67 \times 10^{-3} = 1.14 \times 10^{-3}$ s. From these considerations, we calculate a k_1 of 1890 s^{-1} and a k_2 of 877 s^{-1} (and $1/k_1 + 1/k_2 = 1/600$).

To help interpret these single-molecule data in the context of a bulk, DNA packaging experiment, we consider a general scheme that can describe terminase-catalyzed DNA packaging (Scheme 2). In this scheme, the kinetic step size, m_{kss}, is defined as the average number of base pairs of DNA that are packaged per repeated set of rate constants, $k_1, k_2, ..., k_n$. We note that there are two possibilities here. One is that exactly m_{kss} base pairs of DNA are inserted per set of rate constants, while another is that m_{kss} represents only an average number of base pairs inserted per set of rate constants, such that for a particular occurrence of the set of rate constants $k_1, k_2, ..., k_n$, either more or fewer than m_{kss} base pairs of DNA is actually inserted into the capsid, and the resulting average of this distribution is given by m_{kss}. Using Scheme 2, along with the single-molecule data for λ terminase,

Scheme 2

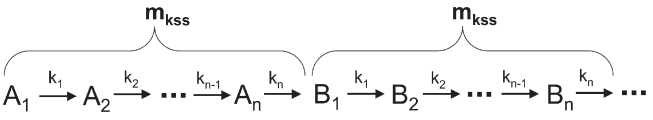

we can see that, on average, we expect 6000 repetitions of two rate-limiting, DNA packaging steps, finally followed by the occurrence of a single slow, pausing step, k_p. Thus, the microscopic rate constants associated with Scheme 2 would be presented as follows: $k_1, k_2, k_1, k_2, ..., k_p$, where the pair k_1, k_2 is repeated, on average, 6000 times, followed by a single occurrence of the slow k_p step. According to Scheme 2, m_{kss} = 6000 bp, k_1 = 1890 s^{-1}, k_2 = 877 s^{-1}, and k_p = 0.36 s^{-1}. With these values, we can use eqs 16 and 17 (see the Appendix for the derivation of these equations) to calculate the apparent values of k_{obs} and m_{obs}, which would correspond to the values that would be obtained if (1) data were generated according to a process governed by Scheme 2 and (2) these data were subsequently analyzed by NLLS methods according to Scheme 1. Thus, the single-molecule data collected for λ terminase, at 23 °C, predict the following bulk kinetic parameters: k_{obs} = 1.66 s^{-1} and m_{obs} = 283 bp. The overall packaging rate constant, including both DNA packaging steps and pausing steps, is $k_{bps} = k_{obs}m_{obs}$ = 469 bp/s. Thus, even though the presence of infrequent pauses during the DNA packaging reaction results in a modest reduction in the overall packaging rate (from 600 bp/s when pauses are specifically edited out of the single-molecule data to 469 bp/s when pauses are included in the data), they result in a very large reduction in the NLLS-derived step size (m_{obs}), from an m_{kss} of 6000 bp to an m_{obs} of 283 bp.

The calculation given above supports our interpretation of the large value we measured for our apparent step size of 410 ± 150 bp. Since this value is too large to correspond directly to a mechanical step size, we suggest this value reflects the presence of pauses in the DNA packaging reaction. We emphasize a direct comparison between the single-molecule data and our bulk, ensemble data is not possible at this time since these two experiments were conducted under very different solution conditions (most notably, our experiments were conducted at 4 °C, while the single-molecule experiments were conducted at 23 °C). However, the calculation given above shows that occasional pauses can indeed result in a large apparent step size, when analyzing DNA packaging data using the *N*-step sequential kinetic model.

Another possible physical interpretation of the m_{obs} of 410 ± 150 bp is that it might represent a process that occurs as the DNA is being spooled into the capsid. For example, the interior diameter of the λ procapsid is ~520 Å; thus, a single turn around the interior of the procapsid would correspond to a distance of $\pi \times 520$ Å (1633 Å). Our value of 410 ± 150 bp corresponds to a contour distance along ds DNA of 1394 ± 510 Å. Therefore, it seems possible this step size might report on the rapid insertion of a single turn of DNA around the interior of the capsid, followed by a slow rearrangement step such that the second step size of DNA can be inserted. However, if this were the case, such regularly spaced events should have been detected in the single-molecule experiments, so we disfavor this interpretation.

To further test our assertion that our packaging data are sensitive to the occasional repetition of a slow step, we have also attempted to analyze our data by forcing *m* to take on values that would be more in line with a mechanical step size. On the basis of the results of Fuller et al. (*1*), we were interested in investigating

the m range of 1−8 bp, where 8 bp corresponds to the upper limit for the mechanical step size based on energetic considerations (*1*). These small values of m result in a much larger number of total steps (N) taken to package the entire DNA length. For N values of > 250, we found that we were unable to use eq 1 to analyze our data, apparently due to computer round-off errors when the ratio of Γ functions is calculated (see Experimental Procedures). To circumvent these problems, we analyzed our data using eq 2, which provides an excellent approximation to eq 1 and is computationally stable, for large values of N.

If we force our global analysis to use values of m from 1 to 8 bp, the resulting fits cannot describe the rapid packaging phase; the best fit simulations are too steep when compared to the experimental data. This can be understood by recognizing that our data provide strong constraints on the overall packaging rate (119 ± 8 bp/s), so that regardless of the value assumed for m, the resulting best fit will provide a value for k_{bps} close to 119 bp/s. For eq 2, the standard deviation of the integrated Gaussian distribution is given by $\sigma = N^{1/2}/k$. Substituting $N = L/m$ and $k = k_{bps}/m$ into the expression for σ, we obtain $\sigma = (Lm)^{1/2}/k_{bps}$. Thus, when m is forced to take on a progressively smaller value, keeping in mind that k_{bps} is well-constrained by the experimental data to a value close to 119 bp/s, the resulting calculated value for σ becomes progressively smaller, resulting in steeper transitions within the rapid packaging phase of the data.

This result indicates that our bulk kinetic data are not reporting solely on the mechanical steps taken by the motor. As discussed above, on the basis of the magnitude of an m_{obs} of 410 ± 150 bp, our data likely report on both pausing and DNA translocation. Thus, m_{obs} can be interpreted as an average value that reports on both of these processes and can be quantitatively understood using eq 17.

We also observe a second, slower phase in our DNA packaging kinetics. We have interpreted this phase as representing at least two populations of complex II, one that is poised to rapidly begin the DNA packaging reaction upon addition of ATP (represented by A in Scheme 1) and the other (represented by NP in Scheme 1) that must first undergo a slow isomerization reaction (given by k_{NP} in Scheme 1) to form A, after which it can begin the DNA packaging reaction. A direct prediction of this model is that both the rate constant, k_{NP}, as well as the fraction of productively bound complexes, x, will be independent of DNA length. Our global, NLLS fitting results are consistent with this prediction. In fact, if we allow k_{NP} and x to vary as local parameters in the NLLS fitting, we observe no obvious trends with an increase in DNA length, again suggesting these parameters are independent of DNA length (data not shown).

Nucleotide Requirements for the Formation of Complex II. We have shown that nucleotide cofactors are required during the *cos* cleavage reaction, for observation of DNA packaging. In the specific case of ADP, we can be confident that this is due to the correct assembly of complex II, which is poised to rapidly begin the DNA pacakging reaction upon addition of ATP. In the case of ATPγS and AMP-PNP, since we have not conducted a detailed kinetic analysis, we are not certain these molecules support formation of complex II. It may be the case that for these latter two molecules, they support correct nicking at *cos*, but then upon addition of ATP, additional slow assembly steps are required before the active packaging compelx is generated. Detailed kinetic studies are required to address these possibilities. Regardless, we have shown conclusively that even though the *cos* site is cut by λ terminase in the presence of Mg^{2+}, in the absence of nucleotides, *cos* processed in this way is unable to support DNA packaging and that this effect cannot be rescued by addition of ADP after cleavage has already occurred in its absence. However, the molecular nature of this requirement is not known. One possibility is that nucleotides are required to support the high-fidelity nicking reaction such that incorrectly nicked DNA cannot be mechanically translocated into the capsid. Another possibility is that nucleotides are required for the proper assembly of the λ terminase packaging machine on the mature left end of the processed *cos* site. We are currently investigating these possibilities in our laboratories.

APPENDIX

Interpretation of Best Fit Parameters k_{obs} and m_{obs} in Terms of the Microscopic Rate Constants Shown in Scheme 2. A general scheme that can describe the kinetics of motor proteins that translocate along their respective lattices is given in Scheme 2. In this scheme, a set of rate constants, represented by k_1, k_2, ..., k_n, are repeated per cycle of the motor protein. For our bacteriophage centric discussion, we consider that m_{kss} base pairs of DNA are packaged into the viral capsid, per set of rate constants, and define m_{kss} as the kinetic step size of the motor (*27*). In Scheme 2, the mechanical step(s) of the motor will correspond to an individual rate constant(s), and the number of base pairs packaged that are associated with the process represented by this rate constant is defined as the mechanical step size (*27*). It is possible more than one of these rate constants may be associated with DNA packaging, such that there may be multiple mechanical step sizes that occur within a single motor cycle.

In practice, regardless of the number of microscopic rates constants present in Scheme 2, the corresponding data (or simulations) can always be very well fitted according to Scheme 1, which corresponds to the classic N-step sequential scheme defined and discussed previously (*19*), yielding apparent average values for k and m, which we will term k_{obs} and m_{obs}, respectively. From m_{obs}, we calculate the apparent average value for the number of steps taken, n_{obs}, while traversing a distance of m_{kss} (one kinetic step size) according to eq 4:

$$n_{obs} = \frac{m_{kss}}{m_{obs}} \tag{4}$$

Our task is to relate these apparent average values, k_{obs} and m_{obs}, to the microscopic steps that are presented in Scheme 2. We begin this discussion by pointing out that regardless of the complexity of Scheme 2, the product of k_{obs} and m_{obs} is a well-constrained fitting parameter and corresponds to the overall translocation reaction velocity, e.g., in units of base pairs of DNA packaged per second:

$$k_{bps} = k_{obs}m_{obs} \tag{5}$$

Thus, if we obtain data that correspond to the translocation of a length of DNA into the interior of the capsid, are specifically monitoring the complete insertion of DNA into the capsid (and not partially packaged intermediates), and analyze these data according to Scheme 1, we can calculate k_{bps} according to eq 5, and this will accurately reflect the overall reaction velocity. To calculate the average time taken by the motor to package m_{kss} base pairs of DNA, we recognize that the expression for the time dependence of the formation and decay of a particular intermediate, say intermediate i, is equivalent to a probability density function. Equation 6 expresses the fraction of a particular

partially packaged intermediate as a function of time, according to Scheme 1:

$$F_i(t) = \frac{(kt)^i}{i!}e^{-kt} \quad (6)$$

where $F_i(t)$ is the fraction of intermediate i packaged, k is the repeated rate constant shown in Scheme 1, and t is the time (*19*). The average and standard deviation of the time distributions associated with packaging the ith intermediate can be calculated in the normal way according to eqs 7 and 8:

$$\mu_i = \frac{\int_0^\infty tF_i(t)\,dt}{\int_0^\infty F_i(t)\,dt} = i/k \quad (7)$$

$$\sigma_i = \frac{\int_0^\infty (t-u_i)^2F_i(t)\,dt}{\int_0^\infty F_i(t)\,dt} = \sqrt{i}/k \quad (8)$$

The average and standard deviation of the amount of time it takes to package one m_{kss} of DNA are given by substituting eq 4 into eqs 7 and 8:

$$\mu_{kss} = \frac{n_{obs}}{k_{obs}} = \frac{m_{kss}}{m_{obs}k_{obs}} \quad (9)$$

$$\sigma_{kss} = \frac{\sqrt{n_{obs}}}{k_{obs}} = \frac{1}{k_{obs}}\sqrt{\frac{m_{kss}}{m_{obs}}} \quad (10)$$

Equations 9 and 10 can be rearranged to provide expressions for k_{obs} and m_{obs} in terms of m_{kss}, μ_{kss}, and σ_{kss}:

$$k_{obs} = \frac{\mu_{kss}}{{\sigma_{kss}}^2} \quad (11)$$

$$m_{obs} = m_{kss}\left(\frac{\sigma_{kss}}{\mu_{kss}}\right)^2 \quad (12)$$

To relate the apparent values of k_{obs} and m_{obs} calculated when using Scheme 1 to analyze data that are in fact reflective of Scheme 2, we have to calculate the expected values of μ_{kss} and σ_{kss}, based on the microscopic rate constants presented in Scheme 2. To calculate μ_{kss} according to Scheme 2, we recognize the total time it takes to complete the set of rate constants (k_1, k_2, ..., k_n) is given by eq 13:

$$\mu_{kss} = \frac{1}{k_1} + \frac{1}{k_2} + \cdots + \frac{1}{k_n} = \sum_{i=1}^{n}\frac{1}{k_i} \quad (13)$$

For example, the total time it takes to package one m_{kss} of DNA is given by the time it takes to complete each substep within the motor cycle. To estimate the standard deviation associated with packaging a single m_{kss} step of DNA, we recognize that the standard deviation associated with each step, k_i, is given by substituting 1 for i in eq 8, which yields eq 14:

$$\sigma_i = \sqrt{1}/k_i \quad (14)$$

The total standard deviation, or equivalently, the total time fluctuations associated with packaging a single m_{kss} of DNA, is then given by adding the standard deviation of each substep in quadrature (analogous to error propagation), which yields eq 15:

$${\sigma_{kss}}^2 = \sum_{i=1}^{n} 1/{k_i}^2 \quad (15)$$

Upon substitution of eqs 13 and 15 into eqs 11 and 12, we obtain expressions (eqs 16 and 17 from the text) that relate the experimentally determined values of k_{obs} and m_{obs} to the microscopic rate constants presented in Scheme 2:

$$k_{obs} = \frac{\sum_{i=1}^{n}\frac{1}{k_i}}{\sum_{i=1}^{n}\frac{1}{{k_i}^2}} \quad (16)$$

$$m_{obs} = m_{kss}\left[\frac{\sum_{i=1}^{n}\frac{1}{{k_i}^2}}{\left(\sum_{i=1}^{n}\frac{1}{k_i}\right)^2}\right] \quad (17)$$

To test the accuracy of eqs 16 and 17, we have simulated time courses according to Scheme 2, using an n of 2−4 (2−4 kinetic steps per cycle), fit the time courses according to Scheme 1 to extract k_{obs} and m_{obs}, and then compared these values with those calculated using eqs 16 and 17. In all cases we have examined, the largest deviation between the fitted and calculated k_{obs} and m_{obs} was 3%.

ACKNOWLEDGMENT

We thank Drs. Michael Feiss and Aaron Lucius for valuable discussions and a careful reading of the manuscript. We also thank Dr. David Bain for helpful discussions.

SUPPORTING INFORMATION AVAILABLE

Additional electrophoresis results. This material is available free of charge via the Internet at http://pubs.acs.org.

REFERENCES

1. Fuller, D. N., Raymer, D. M., Rickgauer, J. P., Robertson, R. M., Catalano, C. E., Anderson, D. L., Grimes, S., and Smith, D. E. (2007) Measurements of single DNA molecule packaging dynamics in bacteriophage λ reveal high forces, high motor processivity, and capsid transformations. *J. Mol. Biol. 373*, 1113–1122.
2. Black, L. W. (1989) DNA packaging in dsDNA bacteriophages. *Annu. Rev. Microbiol. 43*, 267–292.
3. Catalano, C. E. (2000) The terminase enzyme from bacteriophage λ: A DNA-packaging machine. *Cell. Mol. Life Sci. 57*, 128–148.
4. McConnell, M. J., and Imperiale, M. J. (2004) Biology of adenovirus and its use as a vector for gene therapy. *Hum. Gene Ther. 15*, 1022–1033.
5. Rao, V. B., and Feiss, M. (2008) The bacteriophage DNA packaging motor. *Annu. Rev. Genet. 42*, 647–681.
6. Catalano, C. E. (2005) Viral genome packaging machines: Genetics, structure, and mechanism , Kluwer Academic/Plenum Publishers, Georgetown, TX.
7. Maluf, N. K., Gaussier, H., Bogner, E., Feiss, M., and Catalano, C. E. (2006) Assembly of bacteriophage λ terminase into a viral DNA maturation and packaging machine. *Biochemistry 45*, 15259–15268.
8. Maluf, N. K., Yang, Q., and Catalano, C. E. (2005) Self-association properties of the bacteriophage λ terminase holoenzyme: Implications for the DNA packaging motor. *J. Mol. Biol. 347*, 523–542.
9. Rice, P. A., Yang, S., Mizuuchi, K., and Nash, H. A. (1996) Crystal structure of an IHF-DNA complex: A protein-induced DNA U-turn. *Cell 87*, 1295–1306.
10. Chemla, Y. R., Aathavan, K., Michaelis, J., Grimes, S., Jardine, P. J., Anderson, D. L., and Bustamante, C. (2005) Mechanism of force generation of a viral DNA packaging motor. *Cell 122*, 683–692.
11. Fuller, D. N., Raymer, D. M., Kottadiel, V. I., Rao, V. B., and Smith, D. E. (2007) Single phage T4 DNA packaging motors exhibit large force generation, high velocity, and dynamic variability. *Proc. Natl. Acad. Sci. U.S.A. 104*, 16868–16873.

12. Moffitt, J. R., Chemla, Y. R., Aathavan, K., Grimes, S., Jardine, P. J., Anderson, D. L., and Bustamante, C. (2009) Intersubunit coordination in a homomeric ring ATPase. *Nature 457*, 446–450.
13. Smith, D. E., Tans, S. J., Smith, S. B., Grimes, S., Anderson, D. L., and Bustamante, C. (2001) The bacteriophage straight ϕ29 portal motor can package DNA against a large internal force. *Nature 413*, 748–752.
14. Yang, Q., and Catalano, C. E. (2003) Biochemical characterization of bacteriophage λ genome packaging in vitro. *Virology 305*, 276–287.
15. Hang, Q., Woods, L., Feiss, M., and Catalano, C. E. (1999) Cloning, expression, and biochemical characterization of hexahistidine-tagged terminase proteins. *J. Biol. Chem. 274*, 15305–15314.
16. Nash, H. A., Robertson, C. A., Flamm, E., Weisberg, R. A., and Miller, H. I. (1987) Overproduction of *Escherichia coli* integration host factor, a protein with nonidentical subunits. *J. Bacteriol. 169*, 4124–4127.
17. Woods, L., Terpening, C., and Catalano, C. E. (1997) Kinetic analysis of the endonuclease activity of phage λ terminase: Assembly of a catalytically competent nicking complex is rate-limiting. *Biochemistry 36*, 5777–5785.
18. Yang, Q., and Catalano, C. E. (2004) A minimal kinetic model for a viral DNA packaging machine. *Biochemistry 43*, 289–299.
19. Lucius, A. L., Maluf, N. K., Fischer, C. J., and Lohman, T. M. (2003) General methods for analysis of sequential "n-step" kinetic mechanisms: Application to single turnover kinetics of helicase-catalyzed DNA unwinding. *Biophys. J. 85*, 2224–2239.
20. Williams, D. J., and Hall, K. B. (2000) Monte Carlo applications to thermal and chemical denaturation experiments of nucleic acids and proteins. *Methods Enzymol. 321*, 330–352.
21. Grimes, S., Jardine, P. J., and Anderson, D. (2002) Bacteriophage ϕ29 DNA packaging. *Adv. Virus Res. 58*, 255–294.
22. Oliveira, L., Alonso, J. C., and Tavares, P. (2005) A defined in vitro system for DNA packaging by the bacteriophage SPP1: Insights into the headful packaging mechanism. *J. Mol. Biol. 353*, 529–539.
23. Gaussier, H., Yang, Q., and Catalano, C. E. (2006) Building a Virus from Scratch: Assembly of an Infectious Virus Using Purified Components in a Rigorously Defined Biochemical Assay System. *J. Mol. Biol. 357*, 1154–1166.
24. Guo, P., Grimes, S., and Anderson, D. (1986) A defined system for in vitro packaging of DNA-gp3 of the *Bacillus subtilis* bacteriophage ϕ29. *Proc. Natl. Acad. Sci. U.S.A. 83*, 3505–3509.
25. Kondabagil, K. R., Zhang, Z., and Rao, V. B. (2006) The DNA translocating ATPase of bacteriophage T4 packaging motor. *J. Mol. Biol. 363*, 786–799.
26. Yang, Q., Hanagan, A., and Catalano, C. E. (1997) Assembly of a nucleoprotein complex required for DNA packaging by bacteriophage λ. *Biochemistry 36*, 2744–2752.
27. Lohman, T. M., Tomko, E. J., and Wu, C. G. (2008) Non-hexameric DNA helicases and translocases: Mechanisms and regulation. *Nat. Rev. Mol. Cell Biol. 9*, 391–401.
28. Duffy, C., and Feiss, M. (2002) The large subunit of bacteriophage λ's terminase plays a role in DNA translocation and packaging termination. *J. Mol. Biol. 316*, 547–561.
29. Tomka, M. A., and Catalano, C. E. (1993) Kinetic characterization of the ATPase activity of the DNA packaging enzyme from bacteriophage λ. *Biochemistry 32*, 11992–11997.
30. Higgins, R. R., Lucko, H. J., and Becker, A. (1988) Mechanism of cos DNA cleavage by bacteriophage λ terminase: Multiple roles of ATP. *Cell 54*, 765–775.
31. Yang, Q., and Catalano, C. E. (1997) Kinetic characterization of the strand separation ("helicase") activity of the DNA packaging enzyme from bacteriophage λ. *Biochemistry 36*, 10638–10645.
32. Ortega, M. E., Gaussier, H., and Catalano, C. E. (2007) The DNA maturation domain of gpA, the DNA packaging motor protein of bacteriophage λ, contains an ATPase site associated with endonuclease activity. *J. Mol. Biol. 373*, 851–865.